VOL. 17, NO. 5, SEPT.-OCT. 1980 J. SPACECRAFT 425
ARTICLE NO. 79-1668R

A80-075

Free-Flight Rocket Attitude Motion Due to Transverse Vibration

40011
40017

John E. Cochran Jr.*
Auburn University, Auburn, Ala.
and
D.E. Christensen†
U.S. Army Missile Command, Redstone Arsenal, Ala.

Transverse vibration of free-flight rockets prior to end-of-guidance is shown to be a source of significant rigid-body transverse rates of such rockets subsequent to end-of-guidance. This is accomplished through the use of two models of a flexible, spinning, free-flight rocket and optical lever data. The simplest of the two models is composed of two coupled rigid bodies; the other is a fairly detailed modal model. Simulated optical lever data is compared as a means of model validation. The two-body model is used successfully to fit optical lever data and thereby determine the significance of transverse vibrational effects in producing rigid-body transverse angular rates at end-of-guidance.

Introduction

RATHER recently, studies have been initiated[1] with the goal of further improvement in the accuracy of free-flight rockets. Although significant reductions in dispersion of free-flight rockets have been accomplished by utilizing improved manufacturing methods, by using various techniques, such as spinning the rocket to minimize the effects of mechanical thrust misalignment, and by using launchers which provide release of the rocket without producing appreciable tipoff, further improvement in free-flight rocket accuracy will foreseeably require more detailed analysis of factors which were once considered relatively insignificant. One such factor is that of transverse flexibility of the rocket.

Since no structure is perfectly rigid, all rockets are flexible to some extent. In the past, however, most free-flight rockets were designed with length to diameter (L/D) ratios less than, say, 15. Furthermore, the structures of these rockets tend to be dense. Such rockets are so relatively rigid that they can be modeled well as variable-mass rigid bodies.[2] Advances in materials science have, however, presented the free-rocket designer with strong lightweight alloys and composite materials. Free-flight rockets constructed using such materials will, in general, be lighter (warhead excluded) than their predecessors and often more flexible. Furthermore, efficiency in terms of aerodynamic design dictates large L/D rockets which are now structurally *possible* configurations, but which tend to be more flexible than previous rockets with smaller L/D's.

The impact on dispersion of the effects of transverse vibration of a spinning free-flight rocket during the guidance phase *and* its postlaunch motion has not been accurately established. However, a good deal of effort has been expended in the area of determining the effects of flexibility on the stability and control of rockets of the launch vehicle type.[3-5] Also, applied and basic work concerning flexible spinning rockets has been done. In this regard, a paper by Reis and Sundberg[6] addresses the problem of aeroelastic bending of spinning sounding rockets using a simple two-rigid-body model similar to one discussed in the body of this paper, while Womack et. al.,[7] discuss the use of a more complex model based on the use of normal modes to model the flexibility of such rockets. A rather general basic approach to the flexible spinning rocket problem is taken by Meirovitch.[8]

In this paper, free-flight rocket dispersion per se is not considered, but of principal concern is one of the main *contributors* to dispersion, transverse angular velocity of such rockets at the instant of end-of-guidance.[9] As is presently shown, a large fraction of this transverse angular velocity can result from transverse vibration of free-flight rockets during their guidance phases. The problem treated here is different from the problem of modeling the dynamics of a *free*, flexible, spinning rocket because emphasis is placed on the *transition* from constrained motion (during guidance) to free flight.

Different approaches can be taken in modeling the guidance phase to free-flight phase transition of a free-flight rocket; for example, a finite-element method may be used.[10] But such representations, while very good as far as modeling the structure is concerned, often cloud the issue as far as determining the significance of the truly important parameters. In fact, a simple rigid-body model, discussed herein and in Refs. 11 and 12 has been used rather successfully to model the attitude motions of a spinning, flexible, free-flight rocket.

The primary purpose of this paper is to describe certain facets of an effort to determine the effects of transverse flexibility of free-flight rockets on their rotational motion during the guidance phase and the subsequent free-flight phase, up to the time when aerodynamic reactions become significant. Two physical models of a flexible rocket have

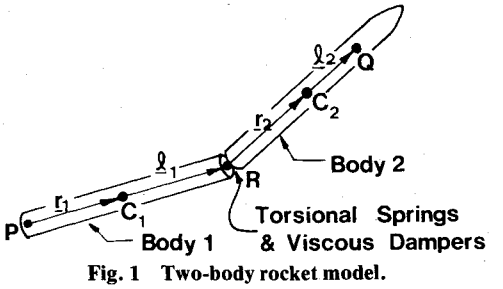

Fig. 1 Two-body rocket model.

Presented as Paper 79-1668 at the AIAA Atmospheric Flight Mechanics Conference, Boulder, Colo., Aug. 6-8, 1979; submitted Nov. 19, 1979; revision received April 14, 1980. This paper is declared a work of the U.S. Government and therefore is in the public domain.
Index categories: LV/M Vibration; LV/M Simulation.

*Alumni Professor, Aerospace Engineering. Associate Fellow AIAA.
†Mechanical Engineer, Launchers and Trackers. Member AIAA.

been adopted: 1) the two-body model, which is the simplest that should give meaningful results, and 2) a much more sophisticated model, which is used primarily to justify the use of the simpler model. The rocket launcher is modeled as nonmoving, since the rockets considered were test rockets fired from a fixed test device. Comparisons of theoretical results with experimental data (optical lever) are made to illustrate the accuracy of the two-body model and to point up the significance of transverse flexibility.

Two-Body Rocket Model

Justification and Description of the Model

Optical lever data which contains evidence of transverse vibration of the tested rocket during its flight generally reveals that the first bending mode is dominant. The rigid-body modes and first free-free bending mode of a flexible rocket can be modeled using two rigid bodies coupled together by linear torsional springs. The appeal of such a model is that it is simple; its justification is found in the fact that the two-body model and a more complex modal model give very nearly the same results, if only first-mode bending is significantly excited.

A sketch of the two-body model is given in Fig. 1. The model is composed of two almost axisymmetric rigid bodies. These bodies are connected at point R in such a manner that the forward body (hereafter called body 2) may rotate relative to the aft body (hereafter called body 1) transversely with respect to the symmetry (if no dynamic imbalance is present) axis of body 1. This relative rotation is elastically restrained and viscous damping is also present.

The point P is located near the aft end of body 1 and the center of mass of body 1, denoted by C_1, is located with respect to P by the vector $\boldsymbol{r}_1$. The vector $\boldsymbol{l}_1$ connects points C_1 and R and the vectors $\boldsymbol{r}_2$ and $\boldsymbol{l}_2$ are directed from R to C_2 (the center of mass of body 2) and from C_2 to Q, respectively. Points P and Q are assumed to correspond to the points at which the rocket is supported while on the launcher.

During the guidance phase, it is assumed that the launcher does not move; therefore, it is referred to as a "rigid" launcher. It follows that while on the launcher the rocket is constrained so that points P and Q translate along a fixed straight line. The motion of the rocket on the launcher is not of particular interest here, except for the fact that P and Q move as stated, because the two-body model is used only in describing motion after end-of-guidance.

During its free-flight phase, a rocket is generally acted on by gravity, aerodynamic reactions, and forces and moments due to the flow internal to the rocket. With a desire to maintain simplicity in our model, however, the mass of the rocket is assumed to be constant during the short period of time of interest and aerodynamic reactions are assumed negligible.

In Ref. 12, a complete derivation of the equations of motion based on the two-body model is given. To keep the length of this paper within acceptable bounds, only a few equations are given here.

The orientation of the rocket's nose is of primary importance because optical lever data provides that information. This orientation is specified by using the coordinate systems shown in Fig. 2. A dextral, orthogonal, coordinate system, $OXYZ$, fixed to the Earth's surface is used as the reference for all motion. A body 1-fixed coordinate system $C_1x_1y_1z_1$, and a corresponding body 2-fixed system $C_2x_2y_2z_2$, are defined such that the x_j axis is the longitudinal geometric axis of body j. The y_2 and z_2 axes lie in the x_1y_1 and x_1z_1 planes, respectively, when the x_1 and x_2 axes are collinear. The system $Cxyz$ is defined such that, although its origin is the center of mass of bodies 1 and 2, its axes are aligned with those of the $C_1x_1y_1z_1$ system.

The angular velocity of the $Cxyz$ coordinate system (and also the $C_1x_1y_1z_1$ system) is $\boldsymbol{\Omega}$, that of the $C_2x_2y_2z_2$ system is $\boldsymbol{\omega}_2$, and that of the $C_2x_2y_2z_2$ system relative to the $Cxyz$ system is $\boldsymbol{\omega}_{2/1}$.

The orientation of the $Cxyz$ system is defined by using the Eulerian angles Ψ, Θ, and Φ in a 3-2-1 rotation sequence as illustrated in Fig. 3. The angles θ_2 and θ_3, also shown, are used to define the relative orientation of body 2. Additionally, to allow for mechanical thrust misalignment effects, the small angles α_y and α_z, where α_z is a rotation about the z_1 axis and α_y is a rotation essentially about the y_1 axis, are introduced. These angles define the orientation of $\boldsymbol{F}_T$, the thrust, with respect to the x_1 axis.

Newton's laws of motion may be applied[12] to derive two nonlinear differential equations for the matrix counterparts of the vectors $\boldsymbol{\Omega}$ and $\boldsymbol{\omega}_{2/1}$ for the free-flight phase. Since aerodynamic reactions are neglected, the rotational and translational motions of the rocket as a whole may be uncoupled. Thus, one can consider separately the rotational motion, which is of primary interest here. The nonlinear equations for $\boldsymbol{\Omega}$ and $\boldsymbol{\omega}_{2/1}$, combined with appropriate kinematic equations for Ψ, Θ, Φ, θ_2, and θ_3, may be solved numerically to obtain time histories of the rotational motions of the two bodies.

The desire for a closed-form solution for the rocket's rotational motion motivated the derivation of linearized versions of the equations of rotational motion. These linear equations generally provide accurate results because the angular deflections and angular rates, except for spin rate, are usually small.

If the assumptions are made that θ_2 and θ_3 are small angles, that $|\dot{\theta}_j| = |\omega_j|$, $j=2, 3$ are small compared to 1 rad/s and that $|\Omega_2|$ and $|\Omega_3|$, the magnitudes of the y and z components of $\boldsymbol{\Omega}$, are also small, then the nonlinear equations can be approximated by a linear matrix differential equation of the form

$$\boldsymbol{I}\dot{\boldsymbol{x}} = \boldsymbol{B}\boldsymbol{x} + \boldsymbol{T} \tag{1}$$

and by the scalar differential equation

$$I_A\dot{\Omega}_1 = T_A \tag{2}$$

Here, $\boldsymbol{I}$ is a constant 6×6 matrix, $\boldsymbol{x} = (\Omega_2\Omega_3\omega_2\omega_3\theta_2\theta_3)^T$ and $\boldsymbol{B}$ is a 6×6 time-varying matrix if T_A, the spin torque, is

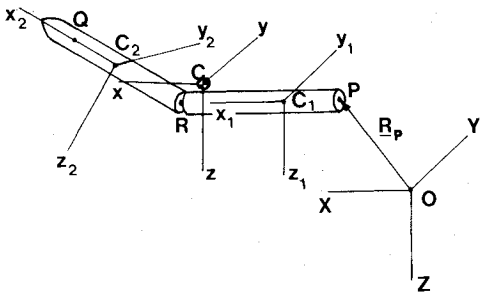

Fig. 2 Coordinate systems used in two-body model analysis.

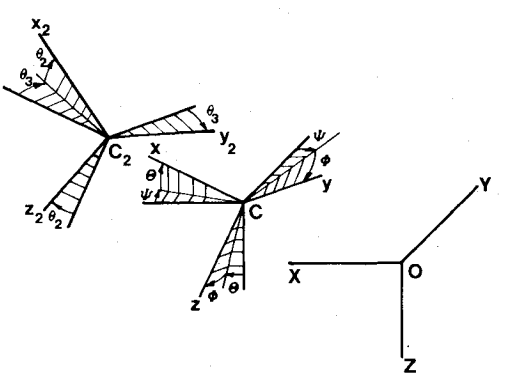

Fig. 3 Orientations of the two bodies.

nonzero. Also, I_A is the axial moment of inertia of the undeformed rocket.

An analytical solution of Eqs. (1) and (2) when T_A is nonzero does not appear possible. Therefore, the choice was made to approximate Ω_1 by a constant, which is the average value of the spin rate during the period of time of interest. For the present, it has also been assumed that the centers of mass of bodies 1 and 2 lie on the axes x_1 and x_2, respectively, and that each body is axisymmetric. The elements of $\boldsymbol{I}$ and $\boldsymbol{B}$ are given explicitly in Ref. 12 for the case incorporating the above assumptions. They contain the moments of inertia, A_1 (B_1) and A_2 (B_2), and mass, m_1 (m_2), of body 1 (body 2), the spin rate Ω_1, the x components of the vectors r_1, l_1, r_2 and l_2 when the angles θ_2 and θ_3 are zero, and the damping c and stiffness k constants of the coupling dampers and springs. The matrix $\boldsymbol{B}$ also contains F_T, the magnitude of the thrust. The matrix $\boldsymbol{T}$ in Eq. (1) is due to mechanical thrust misalignment and has the form

$$T=[-\alpha_y F_T l_C \quad -\alpha_z F_T l_C \quad 0 \quad 0 \quad 0]^T \tag{3}$$

where

$$l_C=[r_1 m_1+(l_1+r_1+r_2)m_2]/[m_1+m_2]$$

When the spin rate $\dot{\Phi}=\Omega_1$ is a nonzero constant, the six scalar equations represented by Eq. (1) are generally coupled. However, since they are time invariant they may be solved by elementary methods.[12] Once the solution for $\boldsymbol{x}(t)$ is obtained, the solutions for $x_1=\Omega_2$ and $x_2=\Omega_3$ may be inserted into the linearized kinematic equations:

$$\dot{\Theta}=\Omega_2\cos\Phi-\Omega_3\sin\Phi \tag{4a}$$

and

$$\dot{\Psi}=\Omega_2\sin\Phi+\Omega_3\cos\Phi \tag{4b}$$

where if t_0 is the "initial" time (as the solution is used here, $t_0=t_{\mathrm{EOG}}$, the time of end-of-guidance), $\Phi=\Omega_1(t-t_0)$. Then, Θ and Ψ can be found by direct integration. Equations (4) are, of course, predicted on the assumption that Θ is small. Hence, either the launch direction is almost horizontal or the $OXYZ$ system does not have its X axis horizontal.

Once Θ, Ψ, θ_2, and θ_3 have been found explicitly,[12] the pitch (Θ_n) and yaw (Ψ_n) angles of the nose of the rocket can be found from the following equations:

$$\Theta_n=\Theta+\theta_2\cos\Phi-\theta_3\sin\Phi \tag{5a}$$

and

$$\Psi_n=\Psi+\theta_2\sin\Phi+\theta_3\cos\Phi \tag{5b}$$

For physical parameters in the range of interest, the solutions for Θ and Ψ contain one mode which is *very lightly* damped even if considerable "internal" damping is included in the equations. This mode has a frequency almost exactly equal to $\lambda=I_A\Omega_1/I_T$, where I_T is the centroidal transverse moment of inertia of the undeformed rocket. The frequency λ should be recognized as the precession frequency of a free axisymmetric rigid body. Since for free rockets $I_A \ll I_T$, this "rigid-body mode" appears for considerable periods of time to be secular rather than periodic.

End-of-Guidance Conditions

Evaluation of the analytical solutions for Θ_n and Ψ_n requires the values of the state variables at end-of-guidance. If it is assumed that points P and Q are translating in the x_L direction at end-of-guidance, these values, indicated by subscript 0, are

$$x_{10}=-(k_1/k_2)\dot{\Theta}_{n0} \tag{6a}$$

$$x_{20}=-(k_1/k_2)\dot{\Psi}_{n0} \tag{6b}$$

$$x_{30}=k_1(\dot{\Theta}_{n0}+\Omega_1\Psi_{n0}) \tag{6c}$$

$$x_{40}=k_1(\dot{\Psi}_{n0}-\Omega_1\Theta_{n0}) \tag{6d}$$

$$x_{50}=k_1\Theta_{n0} \tag{6e}$$

$$x_{60}=k_1\Psi_{n0} \tag{6f}$$

$$\Theta_0=-x_{50}/k_2 \tag{6g}$$

$$\Psi_0=-x_{60}/k_2 \tag{6h}$$

where if

$$d_1=l_1+r_1 \qquad d_2=l_2+r_2 \qquad d=d_1+d_2$$

then

$$k_1=d/d_1 \qquad k_2=d/d_2$$

The Modal Model

Description of the Model

A more sophisticated physical model for a flexible rocket is that of a slender elastic rod which is moving under the influence of gravity, a force which acts at a point on the elastic axis of the rod "interior" to the rod, and a force which acts through the point P with its line of action transverse to the elastic axis at that point. This model is depicted in Fig. 4. The "internal" force has a magnitude equal to that of the thrust and the transverse force is used to model angular thrust misalignments. While the rocket is on the launcher, two points, P and Q, on its elastic axis are constrained to move in the x_L direction only.

The mass distribution and stiffness of the rod are assumed to be functions of the longitudinal coordinate x. The elastic deformations are assumed to be small compared to its length and only transverse deformations are considered to be significant. Furthermore, the rod is assumed to be slender enough (large L/D) that shear deformations and rotary inertia effects are negligible compared to those due to transverse displacement of the elastic axis due to bending.

Equations of Motion

Equations of motion for a flexible rocket based on the slender rod model have been derived, using the Newtonian approach, for both the guidance and free-flight phases.[11,12] These equations are hybrid differential equations; that is, some equations contain both ordinary derivatives of variables such as the angular velocity components of rotating axes and partial derivatives of the elastic deformation variables with respect to time and the longitudinal coordinate. Others contain only ordinary derivatives with respect to time.

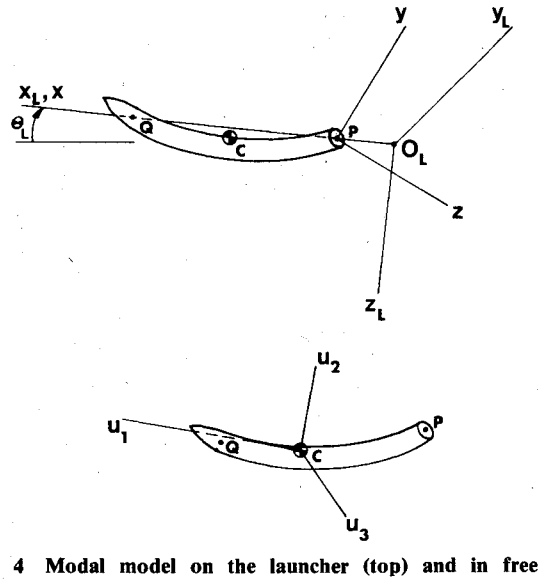

Fig. 4 Modal model on the launcher (top) and in free flight (bottom).

Table 1 Characteristics of two-body model of GEM 7

m_1(kg)	50.466	m_2(kg)	64.286	k(Nt-m)	1.491×10^6
l_1(m)	0.9376	l_2(m)	−0.3354	F_T(Nt)	46720
r_1(m)	0.9376	r_2(m)	0.7393	I_A(kg-m^2)	99.7
Radius (m)	0.095	Radius (m)	0.095	I_A(kg-m^2)	0.406
A_1(kg-m^2)	0.1681	B_1(kg-m^2)	0.1789	Ω_1(rad/s)	47
A_2(kg-m^2)	10.996	B_2(kg-m^2)	5.274	c(Nt-m/s)	13.56

Table 2 Data for modal model of GEM 7

L (m)	3.353
EI (Nt-m^2)[a]	1.652×10^6
$\bar{\sigma}$ (kg/m)[b]	26.93 $(0\le x\le x_M)$
	43.49 $(x_M\le x\le L)$
x_M (m)[c]	1.875
x_Q (m)	2.236
I_A (kg-m^2)	0.406
I_T (kg-m^2)	99.7
F_T (Nt)	46720 $(0.0\le t\le0.25)$
T_A (Nt-m)	284.2 $(0.0\le t\le0.0647$

[a] EI is the model bending stiffness.
[b] $\bar{\sigma}$ is the model mass per unit length.
[c] x_M is the x coordinate of the head end of the motor section.

The elastic motion during guidance is with respect to the rotating reference frame $Pxyz$, the x axis of which passes through point Q. The x axis remains parallel to the x_L axis throughout this phase. During the free-flight phase, the elastic motion is with respect to principal axes u_j of the deformed rocket. The equations for the free-flight phase are very similar to those of Meirovitch.[8]

The hybrid equations have been replaced approximately by ordinary differential equations.[11,12] Normal mode shapes for a slender, uniform beam, pinned at two points, were used to accomplish this for the guidance phase. For the free-flight phase, the normal mode shapes for a free-free, uniform, slender beam were adopted. For both phases, the equations governing the bending vibrations are of the form (n modes)

$$M\ddot{q}+D\dot{q}+Kq=F \tag{7}$$

where M is a $2n\times2n$ generalized mass matrix, q is a $2n\times1$ matrix of generalized coordinates, D is a $2n\times2n$ matrix which contains damping coefficients and terms due to angular rotation of the rocket as a whole, K is a $2n\times2n$ matrix which contains the stiffness characteristics of the rocket as well as terms due to rocket rotation and thrust, and F is a $2n\times1$ matrix of generalized forces.

The attitudes of the $Pxyz$ reference frame and the $Cu_1u_2u_3$ reference frame are determined using what are essentially Euler's equations with "torques" due to vibration and appropriate kinematic equations. Equations similar to Eqs. (6) are used to determine θ_n and Ψ_n, but in them, θ_2 and θ_3 are replaced by the appropriate slopes of the bent rocket's nose.

Transformation Required at Launch

Because different reference frames and mode shapes are used in describing the motion of the rocket during the guidance and free-flight phases, a transformation of variables is required at the instant of launch. Simply put, "initial" conditions on the free-flight phase variables must be determined using the "final" conditions on the guidance phase variables. Here, of course, t_{EOG}, the instant of launch, is the final time for the guidance phase and the initial time for the free-flight phase.

If three mode shapes are used, the conditions that 1) P and Q are not moving transversely at end-of-guidance, and 2) the pitch and yaw angles and their first time rates of change are continuous at end-of-guidance can be enforced. Since three mode shapes were thought to be sufficient, this was done. The details of the transformation can be found in Ref. 12. Briefly,

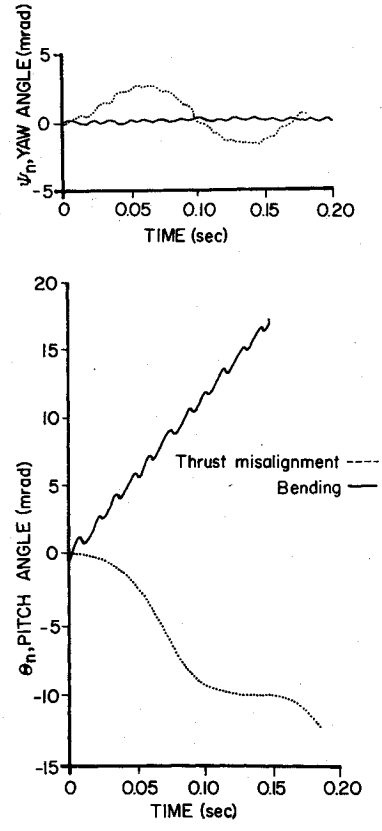

Fig. 5 Two-body model results—separate effects of vibration and thrust misalignment.

the orientation and angular velocity of the principal axes are found at end-of-guidance. These are "initial" conditions for the free-flight phase attitude equations. The conditions enumerated previously are used to find the "initial" conditions for the generalized coordinates which describe the rocket bending after end-of-guidance.

Solution of the Modal Equations

The capability for studying effects of variable spin rate and thrust magnitude is desirable. Because the inclusion of such effects precludes an analytical solution, the modal equations are integrated numerically. Since relatively high frequencies are involved, small time steps are required. Hence, the computer time required to solve the modal equations is an order of magnitude greater than that required to form and evaluate the two-body solutions.

Source of Angular Rates Due to Transverse Vibration

With the model descriptions as background, it is of interest to consider a simple explanation of the "mallaunching" (undesirable angular rates of the rocket at the instant of launch) induced by transverse bending of the rocket. Because the rocket is bent and/or vibrating while on the launcher, its rotational angular momentum H is generally not collinear with the x_L axis or with its instantaneous principal axis of least inertia. Also, while the rocket is on the launcher, con-

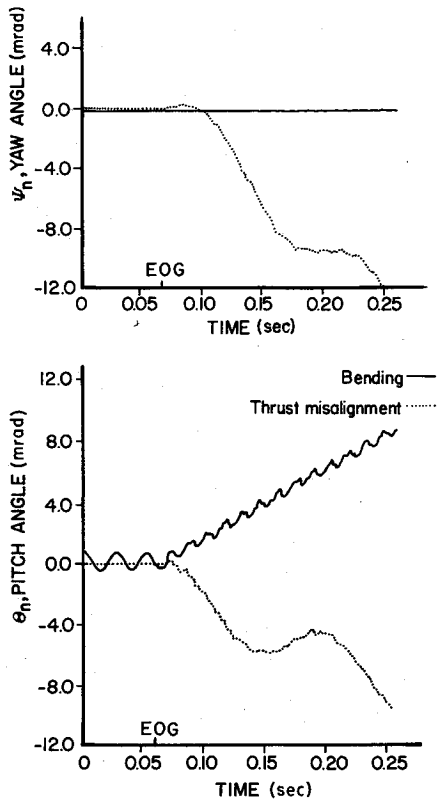

Fig. 6 Modal model results—separate effects of vibration and thrust misalignment.

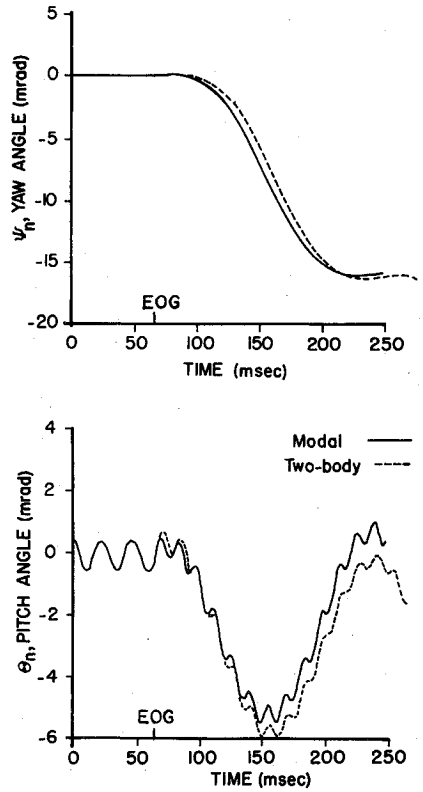

Fig. 7 Comparison of analytical results—combined effects of vibration and thrust misalignment.

straint forces at P and Q change the direction of its rotational angular momentum.

It follows that at the instant of release, the rotational angular momentum of the rocket is generally aligned with neither the x_L nor the u_1 axis. Disregarding thrust misalignment effects until aerodynamic reactions become significant, the vector $\boldsymbol{H}$ of a free-flight rocket is constant. As the rocket rotates in the manner necessary to conserve this angular momentum, it obviously must rotate transversely if there is a transverse component of $\boldsymbol{H}$; hence, "mallaunching" occurs.

Comparison of Analytical Results

To illustrate the effects of transverse vibration on free-flight attitude motion and to show that the two-body model is sufficient for estimating the contributions to observed transverse angular rates made by vibration, some pitch and yaw time histories are presented in this section. The rocket modeled is GEM 7.[13] The physical characteristics of the two-body model are given in Table 1, while the modal model data are in Table 2. The spin rate of GEM 7 was not constant because an eroding spin turbine was used to impart spin. Also, the thrust magnitude was not truly constant. The values given, therefore, are averages. The effects of vibration and of thrust misalignment are considered because optical level data generally contain evidence of both sources of transverse angular rate.

Two-body model results are shown in Fig. 5, where $t_{EOG}=0$. The values $\Theta_{n0}=-0.00025$ rad, $\Psi_{n0}=0.00025$ rad, $\dot{\Theta}_{n0}=0.364$ rad/s, and $\dot{\Psi}_{n0}=0$ were used to obtain the solid curves.‡ The dashed curves were generated by setting all "initial" conditions to zero and putting $\alpha_y=0.000677$ rad and $\alpha_z=0.0045$ rad. When the mean slope of the pitch angle curve is considered, it is obvious that the effect of vibration is *even more significant than that of a large thrust misalignment.*

The vibration-only results shown in Fig. 6 were obtained from the modal model by exciting the first mode of bending in the vertical plane. Because at $t_{EOG}=0.0697$ s (labeled EOG) the pitch and yaw rates of the rocket model's nose were not the same as those cited previously, only qualitative agreement of the two-body model results can be concluded. However, the same values of thrust misalignment angles were used to get the dashed curves shown in Figs. 5 and 6, and very good quantitative agreement between them is apparent.

One important aspect of the modal results in that when significant vibration is present *before* end-of-guidance, there is generally a change in the amplitude of the vibration *at* end-of-guidance. This is because the vibration *after* end-of-guidance is with respect to principal axes of the rocket. Such changes in amplitude are observable in optical lever data.

To obtain a valid comparison of two-body and modal results, the angular orientation and angular velocity of the nose of the modal model at end-of-guidance were used as "initial" conditions for the two-body model solution. The results from both models for the case of combined vibration and thrust misalignment are shown in Fig. 7. Very good quantitative agreement of the results is evident; the main difference is that the mean slope (vibration and thrust misalignment induced nutation averaged out) of the pitch angle time history from the modal model is slightly more negative than its two-body counterpart. Because the vibration and thrust misalignment effects are out of phase in this instance, the slightly more negative slope implies that vibration does not produce quite as much transverse angular rate of the modal model.

Analysis of Optical Lever Data

The two-body model has been used in analyses[11,12] of optical lever data with the objective of determining the significance of transverse vibration of a free-flight rocket in

‡These values were used along with the stated values of thrust misalignment angles to match GEM 7 optical lever data. That is the reason they are not "nice" numbers.

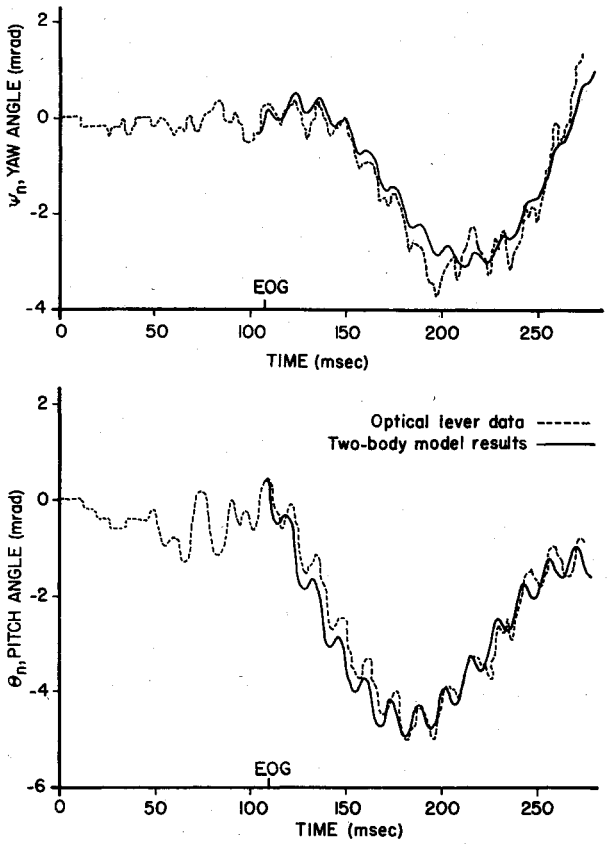

Fig. 8 Theoretical and experimental results for GEM 8—graphical method.

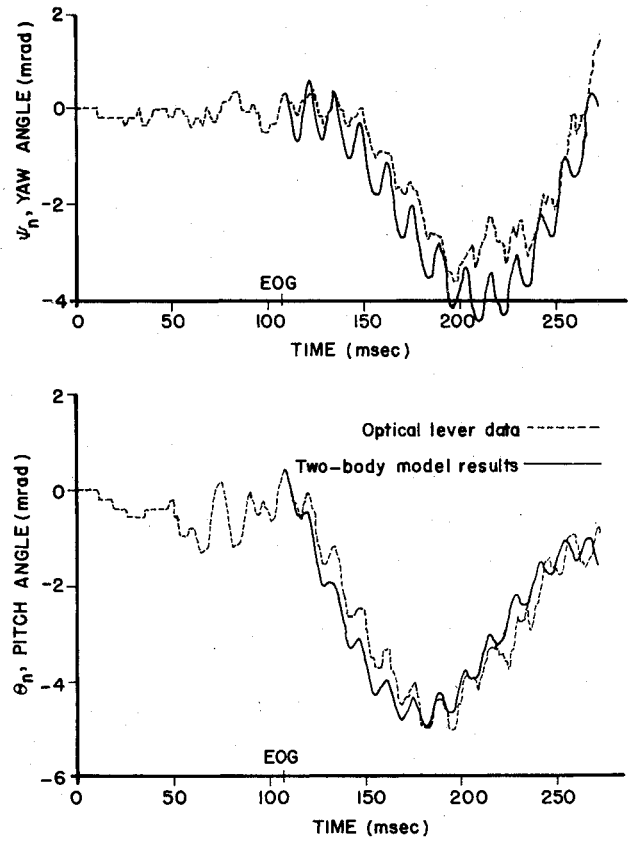

Fig. 9 Theoretical and experimental results for GEM 8—least-squares method.

producing mallaunching. Justification of such use of this model has already been provided.

Two approaches have been used in the analysis. One of these first requires the graphical determination, from optical lever data, of estimates of 1) thrust misalignment present, 2) transverse rotational angular velocity of the rocket with postlaunch bending oscillations neglected, and 3) pitch and yaw angles and angular rates of the nose of the rocket at end-of-guidance. Next, from the end-of-guidance values of the pitch ($\dot{\Theta}_{n0}$) and yaw ($\dot{\Psi}_{n0}$) rates of the rocket's nose, estimates of the transverse angular velocity components ω'_{20} and ω'_{30} of the principal axes of the rocket at end-of-guidance due to vibration are found. The equations used for this purpose are[12] $\omega'_{20}=C\dot{\Theta}_{n0}$ and $\omega'_{30}=C\dot{\Psi}_{n0}$, where

$$C=[(B_2-B_1+\sigma r_2(l_1+r_1))/(I_T-I_A)]k_1-k_1/k_2$$

with

$$\sigma=m_1m_2/(m_1+m_2)$$

To the values of ω'_{20} and ω'_{30} are added angular velocity contributions due to "other" factors such as launcher motion to get the total estimated transverse angular velocity at end-of-guidance.

The other approach is simply to fit the optical lever data with the two-body solution in a least-squares sense. Since the two-body model equations are linear, influence functions for this purpose can be generated by evaluating the solution using a specified initial value on one variable at a time.

By using the "graphical" approach and optical lever data for GEM 8,[14,15] the values, $\Theta_{n0}=0.25$ mrad, $\Psi_{n0}=0$, $\dot{\Theta}_{n0}=-220$ mrad/s, and $\dot{\Psi}_{n0}=140$ mrad/s, were obtained. These were used in the two-body solution to generate the solid curves shown in Fig. 8. The dashed curves were obtained from optical lever data by simply connecting data points with straight lines. Very good agreement between theoretical and experimental results is apparent in Fig. 8.

The physical two-body model for GEM 8 is basically the same as that for GEM 7 (see Table 1). The main differences are small ones in the masses and inertias of the two bodies. Specifically, $I_T=99.5$ kg-m^2, $I_A=0.421$ kg-m^2, $B_1=0.194$ kg-m^2, $B_2=5.088$ kg-m^2, $m_1=50.51$ kg, and $m_2=64.35$ kg. The spin rate used was 30 Hz.

From the above values of model parameters, the value of the constant C is approximately 0.2377. Hence, the transverse angular rate due to vibration of GEM 8 had an estimated magnitude of 71 mrad/s.

The least-squares approach was followed to obtain the solid curves in Fig. 9 by using the optical lever data (22 values of Θ_n and 25 values of Ψ_n). All data used was corrected for bias. The following least-squares estimates were obtained: $\hat{\Theta}_{n0}=0.8722$ mrad, $\hat{\Psi}_{n0}=0.1947$ mrad, $\hat{\dot{\Theta}}_{n0}=-387$ mrad/s, $\hat{\dot{\Psi}}_{n0}=128.5$ mrad/s, $\hat{\alpha}_y=0.685$ mrad, and $\hat{\alpha}_z=3.214$ mrad. The amplitude of the vibration in yaw is smaller than that indicated by the data and in pitch it is larger. Still the agreement is good enough for our stated purpose. By using the values of $\hat{\dot{\Psi}}_{n0}$ and $\hat{\dot{\Theta}}_{n0}$ found through the curve fitting process, an estimated magnitude of the transverse angular rate of GEM 8, due to bending of about 111 mrad/s, was computed. This is higher than the previously given value because allowances for "other" sources of transverse angular rate were not made.

Conclusion

Although physically simple, the two-body model contains the characteristics essential to determining qualitatively and, to a good degree, quantitatively the significance of transverse vibration of a free-flight rocket prior to end-of-guidance in producing transverse rotational motion of the rocket as a whole subsequent to end-of-guidance. Analyses of optical lever data have shown that "mallaunch" rates on the order of 50-100 mrad/s can result from transverse vibration. This is

very significant since mallaunch rates of less than 10 mrad/s are a stated goal for free-flight rocket systems.[1] Causes of vibration and methods of reducing on-launcher vibration and its detrimental effects are currently being studied.

Acknowledgments

This research was performed at Auburn University and Redstone Arsenal under Contracts DAAK40-77-C-0125 and DAAK40-79-C-0030 with the U.S. Army Missile Command.

References

[1] Free Flight Rocket Workshop, U.S. Army Missile Command, Redstone Arsenal, Ala., June 1976.

[2] Cochran, J.E., Jr., "Investigation of Factors which Contribute to Mallaunch of Free Rockets," Final Report on U.S. Army Grant DAHC04-75-0034, Engineering Experiment Station, Auburn University, Auburn, Ala., Jan. 1976.

[3] Beal, T.R., "Dynamic Stability of a Flexible Missile under Constant and Pulsating Thrusts," *AIAA Journal,* Vol. 3, March 1965, pp. 486-495.

[4] Wu, J.J., "Missile Stability Using Finite Elements—An Unconstrained Vibrational Approach," *AIAA Journal,* Vol. 14, March 1976, pp. 313-319.

[5] Meirovitch, L. and Wesley, D.A., "On the Dynamic Characteristics of a Variable-Mass Slender, Elastic Body under High Acceleration," *AIAA Journal,* Vol. 5, Aug. 1967, pp. 1439-1447.

[6] Reis, G.E. and Sundberg, W.D., "Calculated Aeroelastic Bending of a Sounding Rocket Based on Flight Data," *Journal of Spacecraft and Rockets,* Vol. 4, Nov. 1967, pp. 1489-1494.

[7] Womack, W.C., Bert, C.W., and Perdreauville, F.J., "Dynamics of Sounding Rockets at Burnout," *Journal of Spacecraft and Rockets,* Vol. 11, Oct. 1974, pp. 716-720.

[8] Meirovitch, L., "General Motion of a Variable-Mass Flexible Rocket with Internal Flow," *Journal of Spacecraft and Rockets,* Vol. 7, Feb. 1970, pp. 186-195.

[9] Davis, L., Jr., Follin, J.W., and Blitzer, L., *Exterior Ballistics of Rockets,* Van Nostrand Co., Inc., New York, 1958, pp. 102-105 and 314-317.

[10] Cost, T.L. and Weeks, G.E., "Effects of Flexible Rockets and Flexible Launchers on Rocket Launch Conditions Using Finite Elements," *Proceedings of the Third Annual Free Flight Rocket Workshop,* Redstone Arsenal, Ala., Special Rept. T-79-12, Oct. 1978, pp. 112-117.

[11] Cochran, J.E., Jr. and Christensen, D.E., "A Simple Model for Estimating Mallaunch due to Rocket Flexibility," *Proceedings of the Third Annual Free Flight Rocket Workshop,* Redstone Arsenal, Ala., Special Rept. T-79-12, Oct. 1978, pp. 55-98.

[12] Cochran, J.E., Jr., Castleberry, G.A., and Rew, S.D., "An Analysis of the Effects of Transverse Vibration on the Attitude Motion of Free-Flight Rockets," Tech. Rept. RL-CR-80-2, U.S. Army Missile Command, Redstone Arsenal, Ala., Dec. 1979.

[13] "Free Flight Rocket Firing GEM No. 7," U.S. Army Missile Research and Development Command, Redstone Arsenal, Ala., internal memo, Feb. 1976.

[14] "Free Flight Rocket Firing GEM No. 8," U.S. Army Missile Research and Development Command, Redstone Arsenal, Ala., internal memo, March. 1976.

[15] Booker, D.L., "Free Flight Rocket Spin Technique Development," Technical Report T-78-30, U.S. Army Missile Research and Development Command, Redstone Arsenal., Ala., Jan. 1978.